Pakistan J. Zool., pp 1-8, 2022. **DOI**: https://dx.doi.org/10.17582/journal.pjz/20210615060610

Identification of Absorbed Constituents and their Metabolites Related to Estrogen-Like Activity of Total Glycosides of *Cistanche deserticola* in Rat Serum

Yang Hu, Jingxin Ding, Beilei Xu, Xiangming Sun, Guoyu Li, Hui Song, Zheng Zong and Wenlan Li*

College of Pharmacy, Harbin University of Commerce, Harbin 150076, China

Article Information
Received 15 June 2021
Revised 18 July 2022
Accepted 05 August 2022
Available online 08 September 2022 (early access)

Authors' Contribution
Methodology, JD, XS and YH. Validation, HS and ZZ. Data curation, BX and GL. Data analysis, YH. Writing original draft preparation, YH. Writing review and editing, YH and WL. Conceptualization, supervision, project administration and funding acquisition, WL. All authors have read the manuscript.

Key words
Total glycosides of *C. deserticola*, Estrogen-like activity, UPLC-Q-TOF-MS, *in vivo* active compounds, Absorbed constituents

ABSTRACT

Cistanche deserticola Y. C. Ma is a kind of traditional Chinese medicine and food raw material with estrogen-like effect; its active ingredients are glycosides. To explore the absorbed constituents of total glycosides (TGs) *in vivo* and its estrogen-like activity, and reveal its direct acting substances in the body, in this study, 30 female Wistar rats were orally administered with TGs, and serum fingerprints of blood samples collected at 10 different times were established by UPLC-Q-TOF-MS analysis. The estrogen-like activity of TGs was evaluated by determining the proliferation rate of Michigan Cancer Foundation-7 cells. The spectrum-effect relationship was analyzed by serum fingerprint of TGs to characterize the activity *in vivo* and identify the active compounds of TGs. In the results, a total of 75 chemical compounds of TGs were identified in serum, including 11 parent molecules and 64 metabolites. The serum fingerprint of TGs were established, and 36 common peaks were identified. The correlation coefficient and the Grey relational degree between the relative area of the common peaks and the estrogen-like activity of TGs were determined through bivariate analysis and Grey relational analysis, respectively. Total 32 chemical components were identified, including methylated cistantubuloside B, acetylated tubuloside B, and acteoside, which are the active compounds leading to the estrogen-like activity of TGs *in vivo*. In conclusion, this study is expected to provide a theoretical reference for subsequent in-depth studies on the estrogen-like pharmacodynamic material basis of TGs.

INTRODUCTION

Cistanche deserticola Y. C. Ma is a medicinal plant growing in arid or semi-arid areas. Its stem, also known as Rou Cong Rong (Wang *et al*., 2012), is a precious traditional Chinese medicine and is usually used as a tonic (Ai *et al*., 2021; Jiang *et al*., 2009). It can nourish the kidneys, relax the bowels, and protect the liver, exerting anti-oxidant, anti-aging, anti-fatigue, immunoregulation, and estrogen-like effects (Li *et al*., 2020; Piwowarczyk *et al*., 2020; Song *et al*., 2017). It mainly consists of phenylethanol glycosides, iridoids, lignanoids, alkaloids, and polysaccharides (Fu *et al*., 2020; Jiang and Tu, 2009; Tu *et al*., 2007).

During the perimenopause for women, the estrogen levels *in vivo* will decrease, and usually causes adverse reactions such as bone loss, angina pectoris, hot flashes, night sweats, insomnia, dry eyes, dry and aging skin, increased wrinkles, high cholesterol, and memory loss (Bittner, 2009; Ma and Chen, 2015; Zhao *et al*., 2018). Traditional estrogen replacement therapy can treat or alleviate the diseases caused by estrogen deficiency (Rubinow *et al*., 2015; Zetterberg, 2016), however, it is usually accompanied by adverse reactions (Duenas-Garcia *et al*., 2016), increasing the risk of gynecological cancer (Decensi *et al*., 2013). In recent years, researches on phytoestrogen have increased, and found that phytoestrogens have good curative effect on related diseases caused by the decline of estrogen levels with little side effects, and is expected to become an alternative treatment method (Sobenin *et al*., 2016; Tham *et al*., 1998). Studies have compared the effects of a variety of non-hormone drugs treating on perimenopausal symptoms on cardiovascular diseases including blood pressure, heart rate, stroke, incidence rate and mortality, etc., and showed that phytoestrogen had no adverse effects, moreover, it may also reduce the risk of cardiovascular disease through many ways (Mareti *et al*., 2019).

* Corresponding author: lwldzd@163.com
0030-9923/2022/0001-0001 $ 9.00/0

Long-term studies on the estrogen-like activity of *C. deserticola* have been performed to determine the components related to its activity. It has been proved that the total glycosides (TGs) of *C. deserticola* were the active components, and an optimal purification process of TGs had been developed (Li *et al*., 2013, 2019). However, there is still a lack of relevant research on the *in vivo* active compounds of *C. deserticola*, as well as further research on the relationship between the *in vivo* chemical composition of TGs of *C. deserticola* and their estrogenic activity.

In this study, the serum fingerprint of TGs with MCF-7 (commonly used breast cancer cell line) cell proliferation assays were performed to analyze the spectrum-effect relationship of components *in vivo*, and to identify the active compounds of TGs in serum. The findings of this study aims to provide support for the future provide experimental basis for revealing the material basis of estrogen-like effect of TGs, use of *C. deserticola* to alleviate estrogen deficiency in females, and have important implications for the development of *C. deserticola* as a natural functional food.

MATERIALS AND METHODS

Materials, instruments and the preparation of TGs

The dry fleshy stems with scale leaves of *C. deserticola* was made into powder. Then, according to the method of Li *et al*. (2019) and Hu *et al*. (2021), in brief, the *C. deserticola* powder was heated and extracted with 75% ethanol, purified with AB-8 macroporous resin, then eluted with 85% ethanol until it was concentrated into extract under reduced pressure to obtain TGs (62.5%, calculated based on verbacoside). Then, TGs were dissolved in distilled water to create a gavage solution containing 75 mg·mL^{-1} of TGs for subsequent use. The main experimental reagents and instruments were shown in Supplementary Table S1.

Animal groups and administration

Total 30 female Wistar rats (weighing 210 ± 20 g) were housed at 22 ± 2°C with a relative humidity of 50 ± 10%, were adaptively fed for 5 days with free access to food and water. The rats were randomly divided into three groups (n=10): drug group (TGs, crude *C. deserticola dosage* at 18.75 g·kg^{-1}·d^{-1}), positive control group (PC, diethylstilbestrol, 0.35 mg·kg^{-1}·d^{-1}), and blank control group (BC, same volume of distilled water). All groups were administered intragastrically for four consecutive days, twice daily in the morning and evening. Then the rats were fasted but allowed water for 12 h before blood collection.

Blood collection and serum samples

Blood samples (0.5 mL) were collected from the orbital venous plexus for all the groups at 10 different time at 0.25, 0.5, 1, 1.5, 2, 4, 6, 8, 10, and 12 h after the last intragastric administration. After letting stand for 1 h, the serum (supernatant) was obtained by centrifuging at 5000 rpm for 10 min, and stored at −20°C for later use.

Serum samples (200 μL) from the TGs and BC groups were collected, thoroughly mixed with 600 μL of methanol respectively, and centrifuged at 12,000 r·min^{-1} for 10 min. Supernatants were collected, dried with nitrogen, redissolved in 200 μL of 60% methanol, and filtered through a 0.22 μm syringe filter. Thus, 10 serum samples of TGs and BC groups at 10 different time points were obtained for fingerprint and chemical composition analysis, respectively.

UPLC-Q-TOF-MS analysis

The time point with the most transitional components were selected to perform the UPLC-Q-TOF-MS analyze; ACQUITY UPLC BEH C_{18} column (100 mm × 2.1 mm, 1.7 μm) was used, the conditions were according to (Hu *et al*., 2021). Acetonitrile and 0.2% formic acid aqueous solution was used as the solvent system to perform the gradient elution for 20 min. Spectra were recorded in positive and negative ion modes with the scan range of m/z 50-1000. The data were processed and analyzed using Masshunter Qualitative Analysis B.07.00 (Agilent, Santa Clara, CA, USA) (Wu *et al*., 2021).

The *in vivo* and *in vitro* component database of TGs of *C. deserticola* was established by consulting the literature, including the name, molecular formula, molecular weight, CAS and other information of reported known compounds. Molecular structure of target compounds was identified by comparing with reference substances and records in the database based on the analysis of elemental composition, accurate molecular ion mass, fragmentation pattern, and retention time.

Establishment of serum fingerprint of TGs

UPLC-Q-TOF/MS analysis was performed on the serum samples of 10 different time points, the conditions were the same as above. Then, the collected chromatograms were imported into the Similarity Evaluation System for Chromatographic Fingerprint of TCM (version 2004A) software. The peaks with good stability, reproducibility and stable absorption in the serum fingerprint were selected as common peak, and that with large peak area and moderate retention time as the reference peak.

Moreover, the relative retention time and peak area of each common peak was calculated based on the area (set to unity) and retention time (set to unity) of the reference peak, respectively. A methodological research was

performed on the TGS serum fingerprint, the positive and negative ion mode was assessed, including the precision, stability and reproducibility by calculating the relative standard deviation (RSD)(Dou *et al*., 2016b).

MCF-7 cell proliferation assays

Samples (n=10) from each test group were subjected to MCF-7 cell proliferation experiments. MCF-7 cells in logarithmic growth phase were seeded into a 96-well plate at 1.5×10^4 cells/well, 100 μL per well. After incubation for 24 h, cells were treated with serum of BC, PC and TGs groups (5%), respectively. After 72 h, 100 μL MTT was added and incubated for 4 h. Then the culture medium was discarded and 150 μL dimethyl sulfoxide (DMSO) was added to each well, gently shaken for 10 min. The absorbance was measured at 570 nm using a microplate reader, and the average value and proliferation rate were calculated (Ding *et al*., 2019).

Statistical analysis

SPSS 19.0 (IBM, Armonk, NY, USA) was used for bivariate analysis. The Pearson correlation coefficient between the relative peak area of common peaks of serum fingerprints (as the sub sequence) and the proliferation rate of MCF-7 cells (as the parent sequence) was calculated, the grey relational analysis (GRA) was used to calculate their correlation degree (Sun *et al*., 2021).

RESULTS AND DISCUSSION

Chemical composition of TGs in rat serum

To clarify the components and metabolites of TGs in rat serum, UPLC-Q-TOF-MS technology was used to detect the serum samples. In the positive ion mode, total 22 compounds consisting of 4 parent molecules and 18 metabolites were inferred. In the negative ion mode, a total of 53 compounds (excluding the same chemical components as in the positive ion mode) consisting of 7 parent molecules and 46 metabolites were inferred. In total, 75 compounds consisting of 11 parent molecules and 64 metabolites were inferred (Table I, Supplementary Figs. S2 and S3), indicating that TGs mainly exist as metabolites *in vivo*.

Establishing and evaluation of serum fingerprint

The serum fingerprint of TGs were separately established for the positive and negative ion mode (Fig. 1). In the positive ion mode, a total of 22 components were detected. As some components disappeared or had qualitative changes with time, a total of 16 common peaks are finally determined. In the negative ion mode, total 53 components were detected, and finally 20 common peaks were determined. According to the results in Table I, the specific names of the 36 common peaks can be defined.

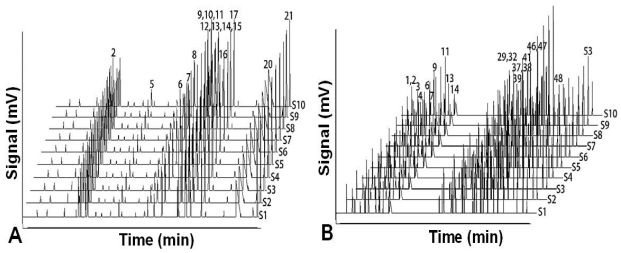

Fig. 1. Serum fingerprint of TGs collected at different time points. (A) positive ion mode; (B) negative ion mode. S1-S10 represent 0.25, 0.5, 1, 1.5, 2, 4, 6, 8, 10, 12 h, respectively.

The methodological performance in positive and negative ion modes was assessed separately using serum samples collected 1 h after intragastric administration. In the positive and negative ion modes, peak 16 (acetylated mussaenosidic acid) and peak 37 (acetylated eucommin A) were selected as reference peaks. The results showed that the RSD was less than 0.2, indicating satisfactory instrumental precision and methodological reproducibility, as well as sample stability within 24 h.

Estrogen-like activity of TGs

In order to clarify the estrogen-like effect of TGs, MCF-7 cell proliferation assays was used to detect the estrogenic activity of serum samples with diethylstilbestrol as the positive drug. In result, the proliferation rate of MCF-7 cells in PC group at all time points was significantly higher than that in BC group (p <0.01, Table II). Compared with BC group, the proliferation rate of MCF-7 cells in TGs group was extremely significant higher at the first 9 time points (0.25, 0.5, 1, 1.5, 2, 4, 6, 8, 10 h) (p <0.01), and significantly higher at the last time point (12 h) (p <0.05). In conclusion, serum samples from TGs group at 10 time points could significantly proliferate MCF-7 cells, indicating that it has estrogen-like activity.

Correlation analysis results

To clarify the components of TGs with estrogen-like effect *in vivo*, the analysis methods combining bivariate analysis and grey correlation were used to correlate the common peak of serum fingerprint with the experimental results of estrogen-like activity. The results showed that (Fig. 2), 13 peaks were detected in positive ion mode correlated with the proliferation rate; in which five peaks showed an extremely significant correlation (Peaks 11, 12, 15, 20, and 21). Eight peaks showed a significant correlation (Peaks 2, 5, 7, 8, 9, 13, 14, and 16). In the negative ion mode, 20 peaks were correlated with the proliferation rate, consisting of 15 peaks with extremely

Table I. Identification of compounds of the characteristic peaks in the serum TGs by UPLC-Q-TOF/MS in positive and negative ion mode.

Ion mode	Peak No.	Retention time (min)	Possible compound	Note	Ion mode	Peak No.	Retention time (min)	Possible compound	Note
+	1	5.031	Acetylated sinapaldehyde glucoside	M	-	17	6.932	Methylated eucommin A	M
+	2	5.197	Acetylated dehydrodiconiferyl alcohol-4-O-β-D-glucoside	M C	-	18	7.967	Geniposide	P
+	3	5.656	Methylated acteoside	M	-	19	8.438	Methylated ononin	M
+	4	6.189	Sinapaldehyde glucoside sulfated conjugate	M	-	20	8.571	Cistanoside F	P
+	5	8.590	Methylated cistantubuloside B	M C	-	21	8.695	Demethylated kankanoside A	M
+	6	11.118	Methylated coniferin	M C	-	22	9.395	8-Epiloganic acid sulfated conjugate	M
+	7	11.698	Dehydrodiconiferyl alcohol-4-O-β-D-glucoside	P C	-	23	9.565	Decaffeoyl acteoside	P
+	8	12.383	Acetylated tubuloside B	M C	-	24	10.155	Acetylated kankanoside I	M
+	9	13.776	Demethylated kankanoside E	M C	-	25	10.992	Kankanoside L sulfated conjugated	M
+	10	13.836	Kankanoside J sulfated conjugate	M C	-	26	11.002	Cistanoside E glucuronidated conjugate	M
+	11	13.869	Methoxylated tubuloside B	M C	-	27	11.068	Acetylated daucosterol	M
+	12	14.459	Acteoside	P C	-	28	11.335	Syringin	P
+	13	14.462	Kankanoside L	P C	-	29	11.674	Acetylated cistanoside G	M C
+	14	14.478	Kankanoside E	P C	-	30	11.723	2-Acetylacteoside glucuronidated conjugate	M
+	15	14.479	Dehydrodiconiferyl alcohol-4-O-β-D-glucoside glucuronidated conjugate	M C	-	31	11.841	Hydroxylated cistanoside G	M
+	16	14.909	Acetylated mussaenosidic acid	M C	-	32	11.847	Methylated tubuloside B	M C
+	17	15.843	Hydroxylated sinapaldehyde glucoside	M C	-	33	12.012	Dehydroxylated kankanoside L	M
+	18	15.876	Acteoside sulfated conjugate	M	-	34	12.019	Ononin	P
+	19	18.037	Kankanoside L glucuronidated conjugate	M	-	35	12.512	Dehydroxylated syringin	M
+	20	18.911	Methylated mussaenosidic acid	M C	-	36	12.573	Kankanoside I glucuronidated conjugate	M
+	21	20.428	Methoxylated coniferin	M C	-	37	12.818	Acetylated eucommin A	M C
+	22	20.794	Tubuloside B glucuronidated conjugate	M	-	38	13.118	Acetylated 2-acetylacteoside	M C
-	1	1.236	Cistanoside G glucuronidated conjugate	M C	-	39	13.144	Hydroxylated ononin	M C
-	2	1.269	3,4-Dihydroxyphenylethanoid glycoside	M C	-	40	13.765	Hydroxylated kankanoside A	M

Table continued on next page.....

Ion mode	Peak No.	Retention time (min)	Possible compound	Note		Ion mode	Peak No.	Retention time (min)	Possible compound	Note	
-	3	1.886	Demethylated (2E,6Z)-8-O-β-D-glucopyranosyloxy-2, 6-dimethyl-2, 6-octadienoic acid	M	C	-	41	13.852	Methoxylated 2-acetylacteoside	M	C
-	4	2.158	8-Epiloganic acid	P	C	-	42	14.086	Dehydroxylated geniposidic acid	M	
-	5	2.765	Methylated salidroside	M		-	43	14.982	Demethylated 8-epideoxyloganic acid	M	
-	6	3.220	Syringin sulfated conjugate	M	C	-	44	15.169	Acetylated geniposidic acid	M	
-	7	3.246	Syringin glucuronidated conjugate	M	C	-	45	15.403	Geniposidic acid sulfated conjugate	M	
-	8	3.313	Syringaresinol-O-β-D-glucopyranoside sulfated conjugate	M		-	46	15.853	Methylated cistanoside E	M	C
-	9	3.646	Acetylated cistanoside E	M	C	-	47	15.903	Methoxylated geniposide	M	C
-	10	4.437	Kankanose	P		-	48	17.277	Methoxylated salidroside	M	C
-	11	4.787	Methoxylated arenarioside	M	C	-	49	17.721	Cistanoside F glucuronidated conjugate	M	
-	12	4.868	Acetylated decaffeoyl acteoside	M		-	50	18.321	Dehydroxylated geniposide	M	
-	13	5.220	Bartsioside sulfated conjugate	M	C	-	51	19.821	Methylated bartsioside	M	
-	14	5.865	Acetylated syringaresinol-O-β-D-glucopyranoside	M	C	-	52	20.443	Salidroside glucuronidated conjugate	M	
-	15	6.004	Methylated kankanoside I	M		-	53	20.872	Methoxylated decaffeoyl acteoside	M	C
-	16	6.788	Demethylated kankanose	M							

P, parent molecule; M, metabolite; C, common peaks; +, positive ion mode; −, negative ion mode.

Table II. Effects of serum TGs collected at different time points on proliferation of MCF-7 cells (n = 10).

Treatment time	Group	A	PR%	Treatment time	Group	A	PR%
0.25 h	BC	0.255±0.043	100.00	4 h	BC	0.258±0.034	100.00
	PC	0.357±0.060**	140.00		PC	0.437±0.037**	169.38
	TGs	0.356±0.035**	139.61		TGs	0.365±0.071**	141.47
0.5 h	BC	0.246±0.051	100.00	6 h	BC	0.273±0.035	100.00
	PC	0.411±0.024**	167.07		PC	0.346±0.053**	126.74
	TGs	0.381±0.056**	154.88		TGs	0.338±0.039**	123.81
1 h	BC	0.296±0.054	100.00	8 h	BC	0.266±0.040	100.00
	PC	0.377±0.023**	127.36		PC	0.431±0.088**	162.03
	TGs	0.367±0.065**	123.99		TGs	0.321±0.040**	120.68
1.5 h	BC	0.294±0.049	100.00	10 h	BC	0.215±0.007	100.00
	PC	0.403±0.051**	137.07		PC	0.373±0.034**	173.49
	TGs	0.377±0.055**	128.23		TGs	0.333±0.029**	154.88
2 h	BC	0.289±0.008	100.00	12 h	BC	0.279±0.032	100.00
	PC	0.402±0.016**	139.10		PC	0.421±0.064**	150.90
	TGs	0.348±0.045**	120.42		TGs	0.332±0.027*	119.00

* p <0.05 and ** p <0.01 in comparison with the blank control group; BC, blank control group; PC, positive control group; TGs, total glycosides of *C. deserticola* administration group; A, absorbance; PR, proliferation rate.

significant correlation (Peaks 1, 4, 6, 7, 9, 11, 14, 29, 32, 37, 38, 39, 46, 48, and 53), and five peaks had a significant correlation (Peaks 2, 3, 13, 41, and 47).

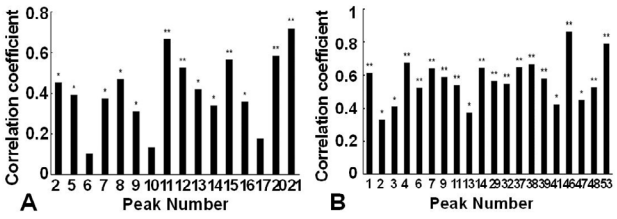

Fig. 2. Bivariate analysis of estrogen activity and common peaks in serum TGs collected at different time points. (A) positive ion mode; (B) negative ion mode.
*significant correlation (p <0.05) when absolute value of correlation coefficient was >0.3; ** extremely significant correlation (p <0.01) when absolute value of correlation coefficient was >0.5.

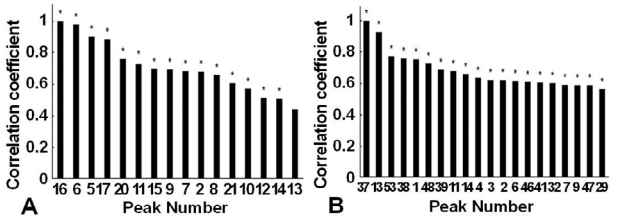

Fig. 3. Grey relational analysis of estrogen activity and common peaks in serum TGs collected at different time points. (A) positive ion mode; (B) negative ion mode.
* correlation when the value of the correlation coefficient was >0.5.

Grey relational analysis was performed, and grey relational degrees between the relative area of each common peak in serum fingerprint of TGs and the estrogen-like activity were calculated. The higher the value, the stronger the relation, with the value above 0.5 indicating a certain level of relation between the sub-sequence and the parent sequence. The results showed that (Fig. 3), 15 peaks in positive ion mode and 20 peaks in negative ion mode were highly correlated with cell proliferation rate.

Overall, 32 common components were identified (Supplementary Fig. S1), including methylated cistantubuloside B; acetylated tubuloside B; acteoside; acetylated dehydrodiconiferyl alcohol-4-O-β-D-glucoside; dehydrodiconiferyl alcohol-4-O-β-D-glucoside; demethylated kankanoside E; methoxylated tubuloside B; kankanoside E; acetylated mussaenosidic acid; dehydrodiconiferyl alcohol-4-O-β-D-glucoside glucuronidated conjugate; methylated mussaenosidic acid; methoxylated coniferin; cistanoside G glucuronidated conjugate; 8-epiloganic acid; syringin sulfated conjugate; 3,4-dihydroxyphenylethanoid glycoside; syringin glucuronidated conjugate; acetylated cistanoside E; methoxylated arenarioside; demethylated (2E,6Z)-8-O-β-D-glucopyranosyloxy-2,6-dimethyl-2,6-octadienoic acid; bartsioside sulfated conjugate; acetylated syringaresinol-O-β-D-glucopyranoside; acetylated cistanoside G; methylated tubuloside B; acetylated eucommin A; acetylated 2-acetylacteoside; hydroxylated ononin; methoxylated 2-acetylacteoside; methylated cistanoside E; methoxylated geniposide; methoxylated salidroside; methoxylated decaffeoyl acteoside. These were inferred to be the active compounds of TGs causing estrogen-like effect *in vivo*.

There have been previous studies on the chemical constituents in *C. deserticola* (Cui *et al*., 2016; Li *et al*., 2015), but they all used *C. deserticola* or some monomer components in *C. deserticola* to analyze the chemical components dissolved in blood. At present, few studies were done on the chemical components of TGs of *C. deserticola*. A relevant study found that *C. deserticola* medicinal serum could significantly promote the proliferation of breast cancer cells (Song *et al*., 2019), which is basically consistent with the results of this study. However, no research on correlation analysis between them. The correlation analysis between serum fingerprints and pharmacodynamic experiments is one of the effective methods to reveal the direct acting substances of drugs *in vivo*. It has been widely used in the material basis research of other traditional Chinese medicine (Dou *et al*., 2016a; Sun *et al*., 2021).

CONCLUSION

In this experiment, UPLC-Q-TOF-MS was used to characterize the components of TGs of *C. deserticola* in rat serum samples after intragastric administration, and a total of 75 chemical components were identified. Bivariate correlation analysis and grey correlation analysis were used, 32 direct acting substances that are highly related to estrogen activity *in vivo* were found in serum in positive and negative ion mode. This study provides a reliable basis for the revelation of TGs estrogen effective substances and their subsequent in-depth development and research.

ACKNOWLEDGMENTS

This study was supported by the Graduate Student Research Innovation Fund of Harbin University of Commerce (No. YJSCX2021-696HSD) and the Key Research and Development Program Guidance Projects of Heilongjiang Province (GZ20210092).

Ethical compliance

All experimental procedures with animals were approved by the Animal Ethical Committee of Harbin University of Commerce (Approval No.: HSDYXY-2018001), following all guidelines, regulations, legal, and ethical standards as required for animals.

Supplementary material

There is supplementary material associated with this article. Access the material online at: https://dx.doi.org/10.17582/journal.pjz/20210615060610

Statement of conflicts of interest

The authors have declared no conflict of interest.

REFERENCES

Ai, Z.P., Zhang, Y., Li, X.Y., Sun, W.L. and Liu, Y.H., 2021. Widely targeted metabolomics analysis to reveal transformation mechanism of *Cistanche deserticola* active compounds during steaming and drying processes. *Front. Nutr.*, **8**: 742511. https://doi.org/10.3389/fnut.2021.742511

Bittner V., 2009. Menopause, age and cardiovascular risk: A complex relationship. *J. Am. Coll. Cardiol.*, **54**: 2374-2375. https://doi.org/10.1016/j.jacc.2009.10.008

Cui, Q.L., Pan, Y.N., Bai, X.W., Zhang, W., Chen, L.X. and Liu, X.Q., 2016. Systematic characterization of the metabolites of echinacoside and acteoside from *Cistanche tubulosa* in rat plasma, bile, urine and feces based on UPLC-ESI-Q-TOF-MS. *Biomed. Chromatogr.*, **30**: 1406-1415. https://doi.org/10.1002/bmc.3698

Decensi, A., Bonanni, B., Maisonneuve, P., Serrano, D., Omodei, U., Varricchio, C., Cazzaniga, M., Lazzeroni, M., Rotmensz, N., Santillo, B., Sideri, M., Cassano, E., Belloni, C., Muraca, M., Segnan, N., Masullo, P., Costa A., Monti, N., Vella, A., Bisanti, L., Aiuto, G.D. and Veronesi, U., 2013. A phase-III prevention trial of low-dose tamoxifen in postmenopausal hormone replacement therapy users: The HOT study. *Annls. Oncol.*, **24**: 2753-2760. https://doi.org/10.1093/annonc/mdt244

Ding, J.X., Li, W.L., Hu, Y., Song, H., Sun, X.M. and Ji, Y.B., 2019. Characterization of estrogenic active ingredients in *Cuscuta chinensis* Lam. based on spectral characteristics and high-performance liquid chromatography/quadrupole time-of-flight mass spectrometry. *Mol. Med. Rep.*, **19**: 1238-1247. https://doi.org/10.3892/mmr.2018.9755

Dou, Z.H., Luo, L., Hou, J.Y., Wang, C.P., Meng, P., Gu, W., and Liu, Q.Q., 2016a. Hepatoprotective ingredients of Yinchenhao decoction based on spectrum-effect relationship of serum containing drugs. *Chin. J. Hosp. Pharm.*, **36**: 1968-1972.

Dou, Z.H., Xu, B., Liu, Q.Q., Gu, W., Meng, P., and Wang, Z.Y., 2016b. Fingerprint of serum containing drug of Yinchenhao decoction. *Chin. Pharm. J.*, **51**: 358-364.

Duenas-Garcia, O.F., Sullivan, G., Hall, C.D., Flynn, M.K. and O'Dell, K., 2016. Pharmacological agents to decrease new episodes of recurrent lower urinary tract infections in postmenopausal women: A systematic review. *Female Pelvic Med. Res.*, **22**: 63-69. https://doi.org/10.1097/SPV.0000000000000244

Fu, Z.F., Han, L.F., Zhang, P., Mao, H.P., Zhang, H., Wang, Y.F., Gao, X.M. and Liu, E.W., 2020. Cistanche polysaccharides enhance echinacoside absorption in vivo and affect the gut microbiota. *Int. J. Biol. Macromol.*, **149**: 732-740. https://doi.org/10.1016/j.ijbiomac.2020.01.216

Hu, Y., Ding, J.X., Sun, X.M., Song, H., Xu, B.L., Qi, Z., Wen, J., Liang, W., Li, W.L. and Ding, Z.D., 2021. Chemical compositions and fragmentation pattern of estrogen effective fraction of *Cistanche deserticola*. *Chin. Pharm. J.*, **56**: 1149-1159.

Jiang, Y., and Tu, P.F., 2009. Analysis of chemical constituents in Cistanche species. *J. Chromatogr. A*, **1216**: 1970-1979. https://doi.org/10.1016/j.chroma.2008.07.031

Jiang, Y., Li, S.P., Wang, Y.T., Chen, X.J. and Tu, P.F., 2009. Differentiation of herb *Cistanches* by fingerprint with high-performance liquid chromatography-diode array detection-mass spectrometry. *J. Chromatogr. A*, **1216**: 2156-2162. https://doi.org/10.1016/j.chroma.2008.04.040

Li, W.L., Chen, Q. Yang, B., and Zhang, J.J., 2013. Screening of phytoestrogenic effective extracts and dose of *Cistanche deserticola*. *Chin. Herb. Med.*, **5**: 292-296. https://doi.org/10.1016/S1674-6384(13)60043-X

Li, W.L., Ding, J.X., Liu, B.M., Zhang, D.L., Song, H., Sun, X.M., Liu, G.Y., Wang, J.Y. and Ji, Y.B., 2019. Phytochemical screening and estrogenic activity of total glycosides of *Cistanche deserticola*. *Open Chem.*, **17**: 279-287. https://doi.org/10.1515/chem-2019-0035

Li, W.L., Sun, X.M., Song, H., Ding, J.X., Bai, J. and Chen, Q., 2015. HPLC/Q-TOF-MS-based identification of absorbed constituents and their metabolites in rat serum and urine after oral administration of *Cistanche deserticola*

extract. *J. Fd. Sci.*, **80**: 2079-2087. https://doi.org/10.1111/1750-3841.12975

Li, Y.Q., Chen, Y., Fang, J.Y., Jiang, S.Q., Li, P. and Li, F., 2020. Integrated network pharmacology and zebrafish model to investigate dual-effects components of *Cistanche tubulosa* for treating both osteoporosis and alzheimer's disease. *J. Ethnopharmacol.*, **254**: 112764. https://doi.org/10.1016/j.jep.2020.112764

Ma, K., and Chen, Y.X., 2015. Discussion on strategy of treatment of perimenopausal syndrome with Chinese and Western Medicine. *China J. Chin. Mater. Med.*, **40**: 3899-3906.

Mareti, E., Ampatzi, C., Paschou, S.A., Voziki E. and Goulis, D.G., 2019. Non-hormonal replacement therapy regimens: Do they have an effect on cardiovascular risk? *Curr. Vasc. Pharmacol.*, **17**: 573-578. https://doi.org/10.2174/1570161116666180911104942

Piwowarczyk, R., Ochmian, I., Lachowicz, S., Kapusta, I., Sotek, Z. and Błaszak, M., 2020. Phytochemical parasite-host relations and interactions: A *Cistanche armena* case study. *Sci. Total Environ.*, **716**: 137071. https://doi.org/10.1016/j.scitotenv.2020.137071

Rubinow, D.R., Johnson, S.L., Schmidt, P.J., Girdler, S. and Gaynes, B., 2015. Efficacy of estradiol in perimenopausal depression: so much promise and so few answers. *Depress. Anxiety*, **32**: 539-549. https://doi.org/10.1002/da.22391

Sobenin, I.A., Myasoedova, V.A., and Orekhov, A.N., 2016. Phytoestrogen-rich dietary supplements in anti-atherosclerotic therapy in postmenopausal women. *Curr. Pharm. Design*, **22**: 152-163. https://doi.org/10.2174/1381612822666151112150520

Song, H., Li, W.L., Liu, B.M., Sun, X.M., Ding, J.X., Chen, N., Ji, Y.B., and Xiang, Z., 2017. Study of the estrogenic-like mechanism of glycosides of cistanche using metabolomics. *RSC Adv.*, **7**: 39403-39410. https://doi.org/10.1039/C7RA06930H

Song, H., Li, W.L., Sun, X.M., Hu, Y., Ding, J.X., Ji, Y.B., and Wang, J.Y., 2019. Estrogenic activity of glycosides from *Cistanche deserticola* as an estrogen receptors adjuvant *in vitro*. *Pharmacogn. Mag.*, **15**: 693-697. https://doi.org/10.4103/pm.pm_402_18

Sun, X.M., Song, H., Zhao, L.Z., Hu, Y., Xin, K.Y., Li, W.L., and Ding, Z.D., 2021. Direct acting substances discovery of estrogen effect of *Cuscuta chinensis in vivo*. *Acta Pharm. Sin.,* **56**: 1826-1831.

Tham, D.M., Gardner, C.D., and Haskell, W.L., 1998. Potential health benefits of dietary phytoestrogens: A review of the clinical, epidemiological, and mechanistic evidence. *Aust. J. clin. Endocr. Metab.*, **83**: 2223-2235. https://doi.org/10.1210/jcem.83.7.4752

Tu, P.F., Shi, H.M., Song, Z.H., Jiang, Y., and Zhao, Y.Y., 2007. Chemical constituents of *Cistanche sinensis*. *J. Asian Nat. Prod. Res.*, **9**: 79-84. https://doi.org/10.1080/10286020500384450

Wang, T., Zhang, X.Y., and Xie, W.Y., 2012. *Cistanche deserticola* Y. C. Ma, Desert Ginseng: A review. *Am. J. Chin. Med.*, **40**: 1123-1141. https://doi.org/10.1142/S0192415X12500838

Wu, X.F., Xie, W., Huang, X.L., Wu, H.Q., Huo, Y.P. and Zhou, X., 2021. Rapid analysis compositions of processed *Citrus medica* L. var. *sarcodactylis* Swingle by UPLC-Q-TOF MS. *J. Chin. Mass Spectrom. Soc.*, **42**: 207-217.

Zetterberg, M., 2016. Age-related eye disease and gender. *Maturitas*, **83**: 19-26. https://doi.org/10.1016/j.maturitas.2015.10.005

Zhao, D., Guallar, E., Ouyang, P., Subramanya, V., Vaidya, D., Ndumele, C.E., Lima, J.A., Allison, M.A., Shah, S.J., Bertoni, A.G., Budoff, M.J., Post, W.S., and Michos, E.D., 2018. Endogenous sex hormones and incident cardiovascular disease in post-menopausal women. *J. Am. Coll. Cardiol.*, **71**: 2555-2566. https://doi.org/10.1016/j.jacc.2018.01.083

Pakistan J. Zool., pp 1-8, 2022. **DOI**: https://dx.doi.org/10.17582/journal.pjz/20210615060610

Supplementary Material

Identification of Absorbed Constituents and their Metabolites Related to Estrogen-Like Activity of Total Glycosides of *Cistanche deserticola* in Rat Serum

Yang Hu, Jingxin Ding, Beilei Xu, Xiangming Sun, Guoyu Li, Hui Song, Zheng Zong and Wenlan Li*

College of Pharmacy, Harbin University of Commerce, Harbin 150076, China

Supplementary Table S1. List of main materials and instruments used in this study.

Materials and instruments	Manufacturers or Sources
Diethylstilbestrol (purity: ≥98%)	Hanpu Pharmaceutical Co., Ltd., Guangzhou, China
Mass spectrometry (MS)-grade formic acid, acetonitrile, methanol	Fisher Scientific, Fair Lawn, NJ, USA)
Phenol red-free RPMI 1640	HyClone, Logan, UT, USA
MTT, DMSO	Sigma-Aldrich, St. Louis, MO, USA
Agilent 1290 HPLC system, Agilent 6530 series quadrupole time-of-flight LC/MS system	Agilent Technologies, Inc., Santa Clara, CA, USA
ACQUITY UPLC BEH C_{18} column (100 mm × 2.1 mm, 1.7 μm)	Waters Crop., Jakarta Selatan, Indonesia
Genius N118LA nitrogen generator	Peak Scientific, Glasgow, UK
Microplate reader	Bio-Rad, Inc., Hercules, CA, USA
The electronic analytical balance AR1140	Ohaus Corporation, Parsippany, NJ, USA
XW-80A vortex mixer	Yugong Machinery Technology Co., Ltd., Shanghai, China
Raw material of dry *Cistanche deserticola*	purchased from Sankeshu Medicinal materials market, Harbin, China
Wistar rats (weighing 210 ± 20 g)	from Harbin Medical University, Harbin, China
MCF-7 cell line	from Research Center of Pharmaceutical Engineering and Technology, Harbin University of Commerce, Harbin, China

* Corresponding author: lwldzd@163.com
0030-9923/2022/0001-0001 $ 9.00/0

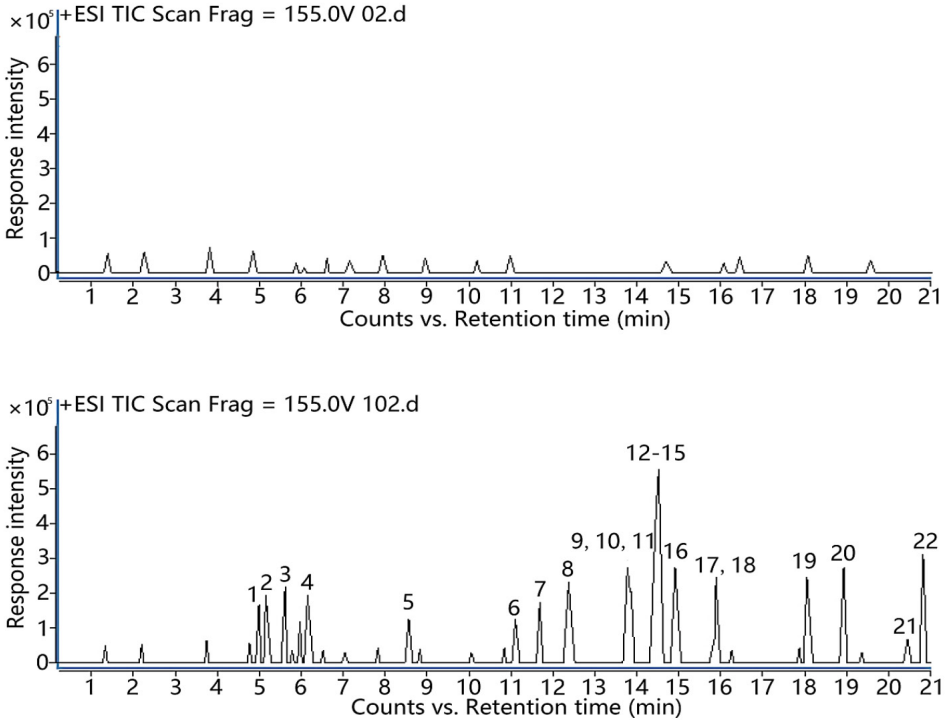

Supplementary Fig. S1. Total ion chromatogram in the positive ion mode. A: blank serum; B: TGs-containing serum.

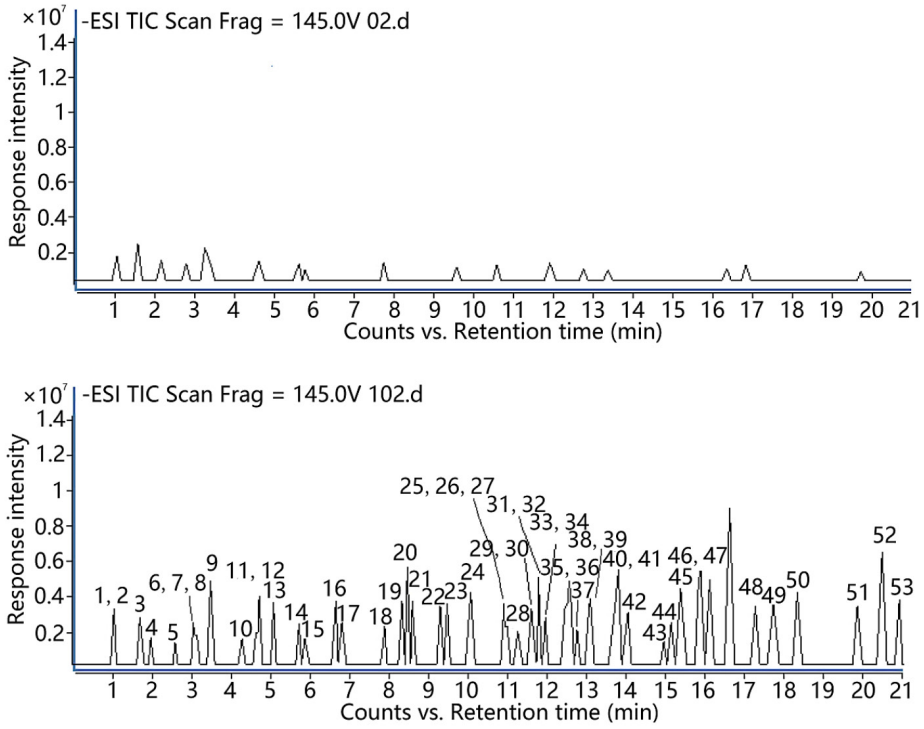

Supplementary Fig. S2. Total ion chromatogram in the negative ion mode. A: blank serum; B: TGs-containing serum.

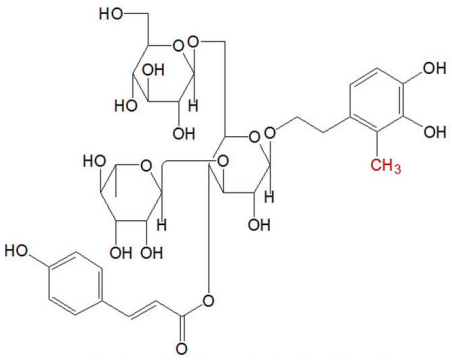

methylated cistantubuloside B

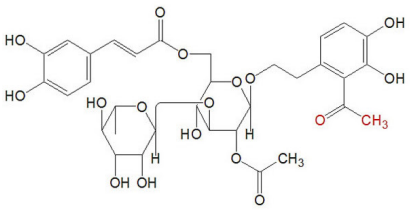

acetylated tubuloside B

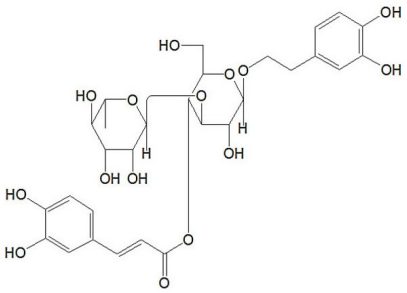

acteoside

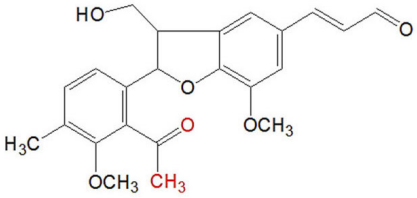

acetylated dehydrodiconiferyl alcohol-4-O-β-D-glucoside

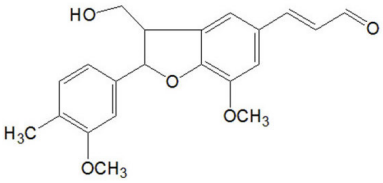

dehydrodiconiferyl alcohol-4-O-β-D-glucoside

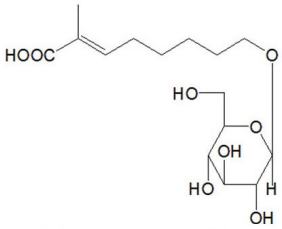

demethylated kankanoside E

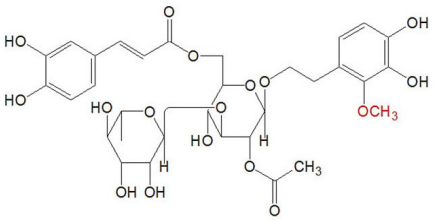

methoxylated tubuloside B

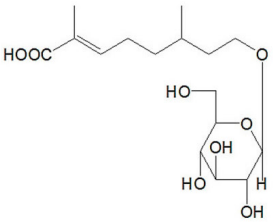

kankanoside E

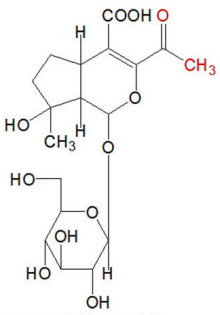

acetylated mussaenosidic acid

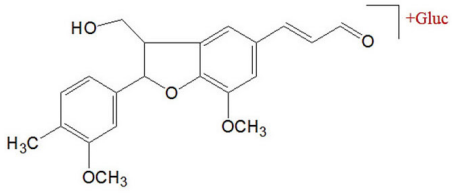

dehydrodiconiferyl alcohol-4-O-β-D-glucoside glucuronidated conjugate

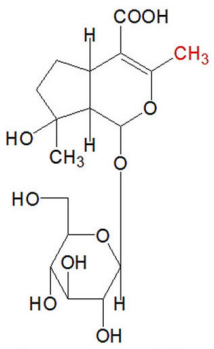

methylated mussaenosidic acid

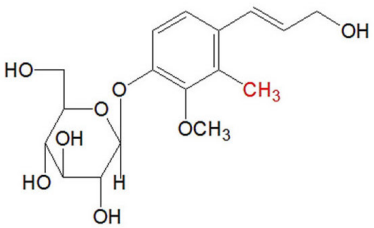

methoxylated coniferin

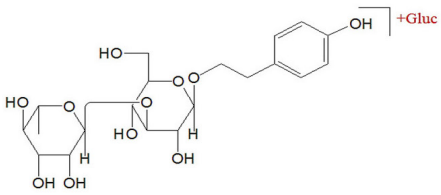

cistanoside G glucuronidated conjugate

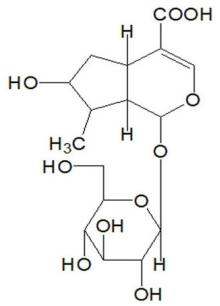

8-epiloganic acid

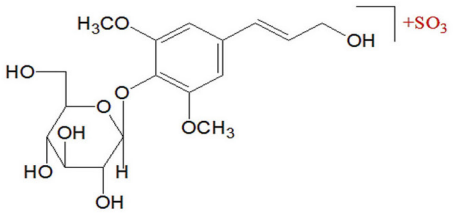

syringin sulfated conjugate

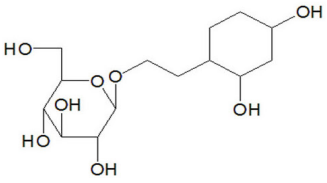

3,4-dihydroxyphenylethanoid glycoside

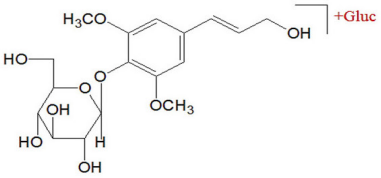

syringin glucuronidated conjugate

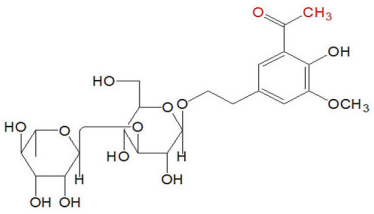

acetylated cistanoside E

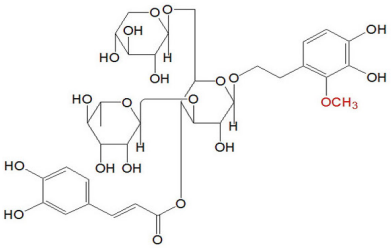

methoxylated arenarioside

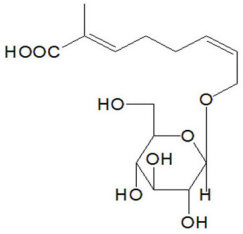

demethylated (2E,6Z)-8-O-β-D-glucopyranosyloxy-2,6-dimethyl-2,6-octadienoic acid

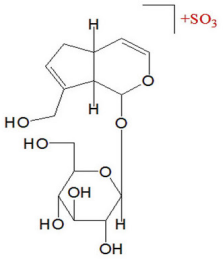

bartsioside sulfated conjugate

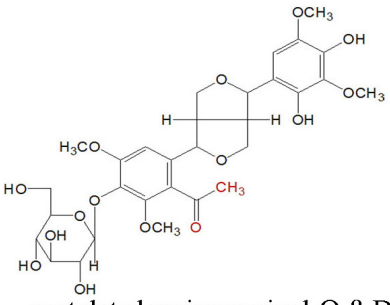

acetylated syringaresinol-O-β-D-glucopyranoside

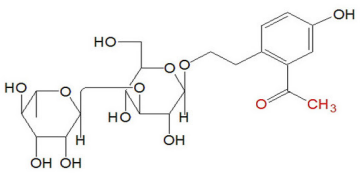

acetylated cistanoside G

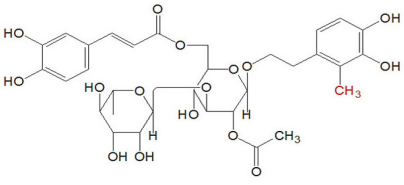

methylated tubuloside B

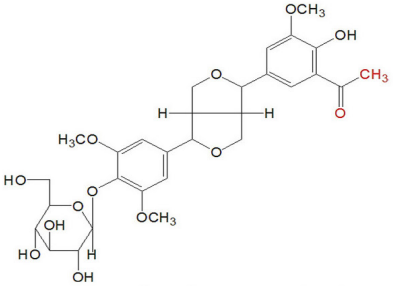

acetylated eucommin A

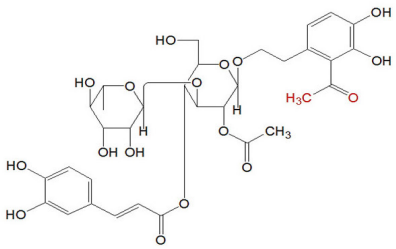

acetylated 2-acetylacteoside

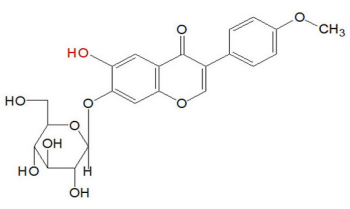

hydroxylated ononin

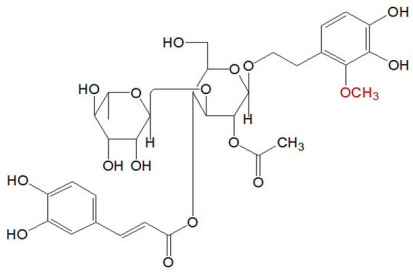

methoxylated 2-acetylacteoside

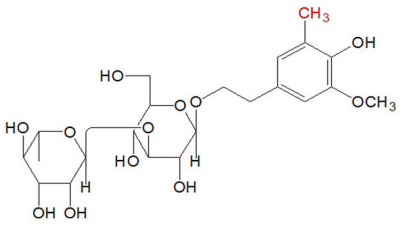

methylated cistanoside E

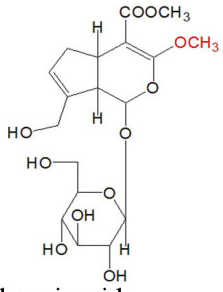

methoxylated geniposide

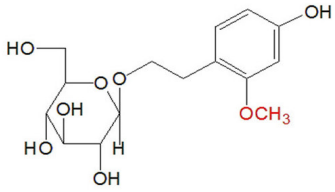

methoxylated salidroside

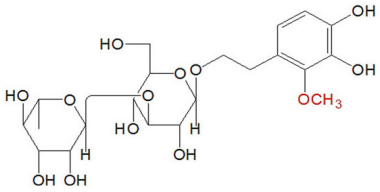

methoxylated decaffeoyl acteoside

Supplementary Fig. S3. *In vivo* active compounds leading to the estrogen-like activity of TGs.